

PCM cool roof systems for mitigating urban heat island - an experimental and numerical analysis

Young Kwon Yang^a, Min Young Kim^a, Min Hee Chung^b, Jin Chul Park^{b,*}

^a Graduate School, Chung-Ang University, Seoul, Republic of Korea

^b School of Architecture and Building Science, Chung-Ang University, Seoul, Republic of Korea

ARTICLE INFO

Article history:

Received 31 May 2019

Revised 9 September 2019

Accepted 17 October 2019

Available online 18 October 2019

Keywords:

Urban heat island mitigation

Phase change material (pcm)

Cool roof

Experimental investigation

Numerical modeling

ABSTRACT

The purpose of this study is to develop a “PCM cool roof system”, and to evaluate its performance by applying the PCM cool roof system to the roof envelop. The study methods and procedures are as follows: First, the optimal PCM and finish materials were selected utilizing the indoor artificial climate chamber. Second, the PCM cool roof system was applied to the testbed, and the changes in surface temperatures were measured to determine the effect on the reduction of the heat island phenomenon. Third, the air currents in Gangdong-gu Seoul Korea were analyzed through a numerical analysis based on the data derived from the testbed to verify the reduction in the UHI. The experimental groups were set to A: WPC, B: WPC+PCM, and the control group to C: PCM cool roof system in the testbed experiment. The experimental environments were divided into winter, intermediate, and summer periods to increase the performance evaluation reliability in Seoul, where there are four distinct seasons. The study results showed that all seasons saw an effect of a reduction of roof surface temperatures when using the PCM cool roof system. The maximum temperature difference for each season was 2.5 °C in winter, 4.7 °C in intermediate season, and 5.7 °C in summer. The a numerical analysis results showed that the reduction in roof surface temperature due to the “PCM cool roof system” was effective in the mitigation of the heat island phenomenon.

© 2019 Published by Elsevier B.V.

1. Introduction

An urban heat island (UHI) is a phenomenon that shows a temperature difference of more than 2 °C between the urban and suburban areas [1]. The main causes of the UHI are increase in population and concrete cover, as well as heat sources generated in the urban areas. The term was used to explain the temperatures in London by Luke Howard in 1820 for the first time. Later, W. Schmitz Wien, an Austrian meteorologist, studied a temperature distribution, and found that a temperature became higher as observations became closer to the urban area [2–4]

Since the UHI influences the micro-climate in urban areas significantly, it prevents pollutants generated in that urban area from being diffused, as well as preventing clean and fresh air in suburban areas from entering to the urban area [5]. The mean temperature of Seoul has also increased by 1.19 °C since 1960, and it was statistically found that the increase was closely related to rapid urbanization. Previous studies discovered that when the building

density in a city is increased by 10%, the temperature in the urban area increased by 0.16 °C [6–8].

In recent years, much attention has been paid to the problem of UHI, so that studies on the causes of UHI and solutions have been conducted in various ways. Some of the typical measures taken to reduce the UHI are the increase of green space and the creation of a wind flow path, and an increase in reflectance from the in urban area in general. The UHI can be mitigated by 2–3 °C on average when these measures are taken [9]. A variety of studies on other methods to reduce the UHI have also been conducted [10–12]. Fig. 1 and Fig. 1.2 shows the Seoul temperature comparisons between 2005 and 2012. It can be confirmed that the temperature has risen in urban areas.

Due to the studies mentioned previously, some major cities around the world, such as London, Paris, Los Angeles, Chicago, Philadelphia, and New York have set and enforced guidelines to reduce the urban heat island protocol. Seoul, South Korea is also well-known metropolitan city whose spatial area is 605.25 km² and has a population of 10.20 million people as of 2016. However, no appropriate measures have been proposed to reduce the UHI yet. It is also not appropriate to apply study results regarding other cities to Seoul, because Seoul has various unique differences, such

* Corresponding author:

E-mail addresses: dora84@naver.com (Y.K. Yang), kmyhg@naver.com (M.Y. Kim), mhloveu@cau.ac.kr (M.H. Chung), jincpark@cau.ac.kr (J.C. Park).

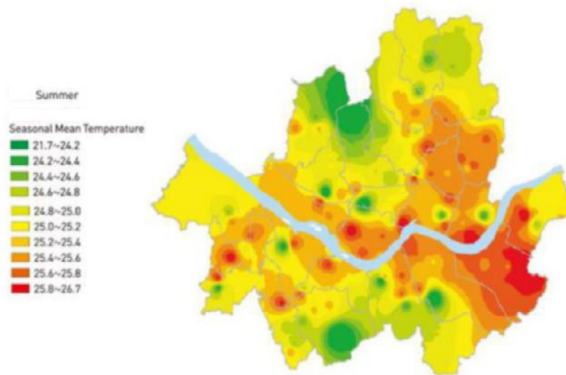


Fig. 1. Seoul average temperature in 2005.

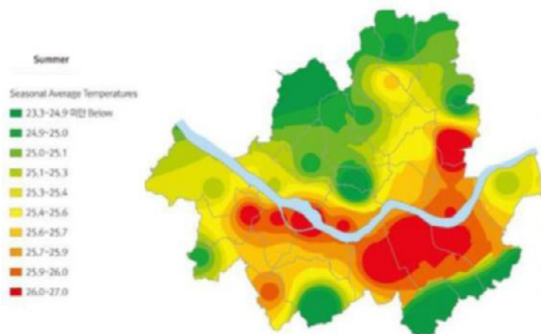


Fig. 2. Seoul average temperature in 2012.

as a high urbanization ratio, development type, and geographical and climate differences.

Studies on the reduction in UHI in Seoul, Park et al. [13], analyzed the effects of the cool roof by taking measurements before and after installation, and Jeong et al. [4], utilized Automatic Weather System (AWS) data to analyze the intensity of the heat island in Seoul (See Fig. 3), and the effects of the reducing the UHI according to complex type and reflectance. A study analyzed the temperature change due to an increase in green space in downtown Seoul [14]. A study on the characteristics of the UHI in Seoul using local analysis system was also published [15].

As described above, much effort has been made to reduce the UHI by the implementation of diverse methods. This study is also dedicated to the same purpose—reduction of the UHI. It aims to lower the surface temperature of building roofs by utilizing a phase-change material (PCM) and to verify the reduction in the UHI.

In a notable study on the reduction of the UHI using phase change materials, Chung and Park [16] conducted a study on the reduction in surface temperature according to applying a PCM tile roof finish, cool paint, a green waterproof finish, and a gray waterproof finish through scaled-down model experiments. They conducted analysis by placing PCM over general tiles and the study results showed that a combination of PCM tile and cool paint was the method best to reduce surface temperatures. Yang et al. [17] verified the reduction of the roof surface temperature and the indoor temperature by applying the PCM to the scaled-down model, and conducted an analysis on the temperature distribution simulation to verify the reduction in temperature on the roof surface and at the urban canopy layer. Karlessi et al. [18] fabricated PCM tiles (six different colors) with different concentrations to

measure surface temperature. Among the studies mentioned above, a number of other studies on utilization of PCM have already been conducted and others are still underway.

Although the results of the previous studies proved that PCM was effective in reduction of the roof surface temperature in buildings, their PCM sizes were small, and used only on scaled-down models (600 mm × 600 mm) or proved the effective by applying PCM to small portion of the roof surface. Thus, no studies have been conducted on the reduction of not only in the roof surface temperature, but also the indoor temperature in the entire building. Previous studies have been focused only on the source technology without the consideration of commercialization. Thus, this study aims to develop a PCM cool roof system and prove the effectiveness of the system on the reduction of the UHI through performance verification by applying the system to a test bed that simulates an actual building. This study also aims to verify the effect of a reduction of the indoor temperature of the building.

2. Materials and methodology

In this study, experiments using an indoor artificial climate test chamber, a testbed application, and a CFD analysis were conducted to verify the performance of the PCM cool roof system that can not only reduce the UHI, but also decrease the cooling loads in buildings through the reduction of the roof surface temperature in buildings.

There are largely four main analysis methods on the UHI: site measurements (Ripley et al. [19]; Arnfield et al. [20]), thermal remote sensing (Voogt et al. [21]; Kim et al. [7]), fabrication of urban scaled-down models (Uehara et al. [22]; de La Flor et al. [23]), and computer simulations (Mirzaei et al. [24]; Roman et al. [25]). In this study, the analysis methods of the fabrication of an urban scaled-down model, site measurements, and computer simulations were conducted. The purpose of this study is to demonstrate the effect of reducing the heat island phenomenon. To do this, we measured the roof surface temperature change through artificial climate experiment, test-bed application experiment and CFD analysis. This study has the following methods and procedures to analyze the effect of PCM on the reduction in the UHI.

- Step 1: A thermal behavior analysis was conducted in the indoor artificial climate test chamber. PCMs requires packing to prevent leakage, due to the characteristic of a phase change from a liquid to a solid state, and also appropriate strength, durability, and heat conductivity to be used as a roof finish material. Thus, proper finish materials and PCMs were selected accordingly.
- Step 2: The PCM cool roof system was fabricated and a testbed application test was conducted. The test was conducted on the rooftop of an office building located in Dongjak-gu, Seoul where the PCM cool roof system was applied. The changes in the surface temperature depending on the roof finish materials during all four seasons (spring, summer, autumn, and winter) were measured.
- Step 3: The effects on the reduction in the heat island phenomenon were analyzed, according to the surface temperature of the roof, through a computational fluid dynamics (CFD) analysis. The data of changes in the surface temperature on the roof, derived in “Step 2”, were used for the analysis.

2.1. Materials

Since a PCM is changed to a liquid state during a phase change, packing is needed to prevent leakage, and a PCM also requires appropriate strength and durability that can be used as a roof fin-

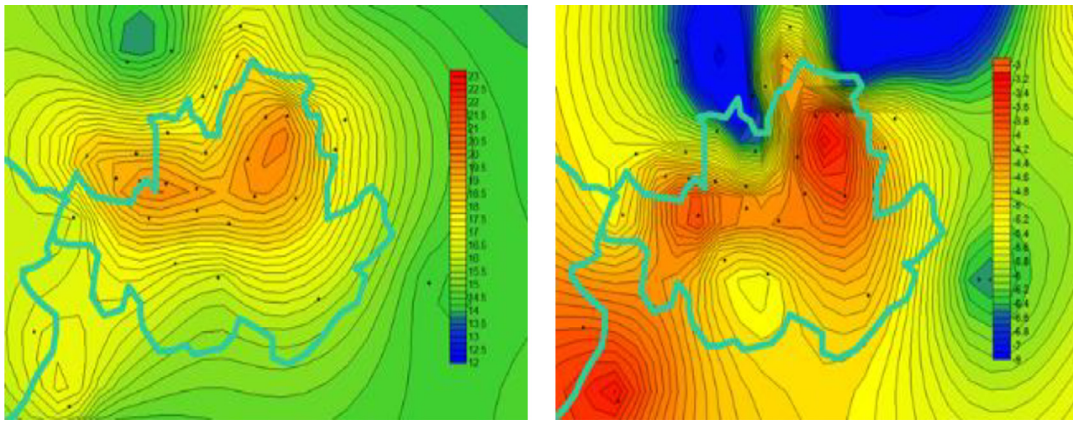


Fig. 3. Analysis of heat island strength in Seoul (AWS).



Fig. 4. Wood plastic composite.

ish, and heat conductivity by which appropriate heat can be transferred to the PCM. Although finishes for roof are various, the PCM cool roof system needs a cavity space where PCM packing can be inserted allowing it to be applied to the existing building conveniently. Thus, finishes that are relatively difficult to form a cavity space in, such as roofing tiles and asphalt shingles were excluded. WPC, wood, and concretes finished rooves were selected. The heat conductivity of the selected materials was measured by the afore mentioned method. The concrete was finally excluded from the finishes, because it requires additional construction work thus the PCM material is difficult to apply conveniently. The general (hard and soft) wood was also excluded due to relatively disadvantageous properties in durability and strength. Thus, WPC was selected as the final finish as the appropriate finish and its detailed heat conductivity was measured. The WPC used in the heat conductivity measurement is shown in Fig. 4. WPC used PT1001E of 'P' company which is an off-the-shelf product. This product is brown, synthetic material made by mixing 30% HDPE(High density polyethylene) and 10% chemical additive in 60% of natural wood powder & fiber. Chemical additives include antioxidants, stabilizers, colorants, antifungal agents, and reinforcing agents(PROTIMBER, 2018).

2.2. Experimental conditions of the indoor artificial climate test chamber

To select an appropriate PCM, which will be inserted to the PCM cool roof system, a similar environment with that of Seoul in summer in terms of average solar radiation was created in the artificial climate test room (8 m^3) to conduct a thermal behavior analysis. The artificial climate test room was composed of two sets of two 650W halogen lamps and an internal reflective screen that surrounded the entire in four directions. The light source type was a lamp for photo shooting that was called FBE and DWE. The solar radiation was selected by comparing the daily mean solar radiation in the standard weather data for summer (June to August) and the maximum solar radiation. The solar radiation was controlled through the dimming control. The solar radiation for each step was checked using a pyrheliometer. The solar radiation during the test satisfied the 5100 W/m^2 average by controlling the solar radiation based on the test representative value thereby ensuring the validity of the artificial climate test room. Additionally, the indoor temperature was maintained at around $30 \text{ }^\circ\text{C}$ (See Fig. 5., Table 1).

Since this study aimed to analyze the thermal performance of the PCM when applied to a highly reflective surface, such as the

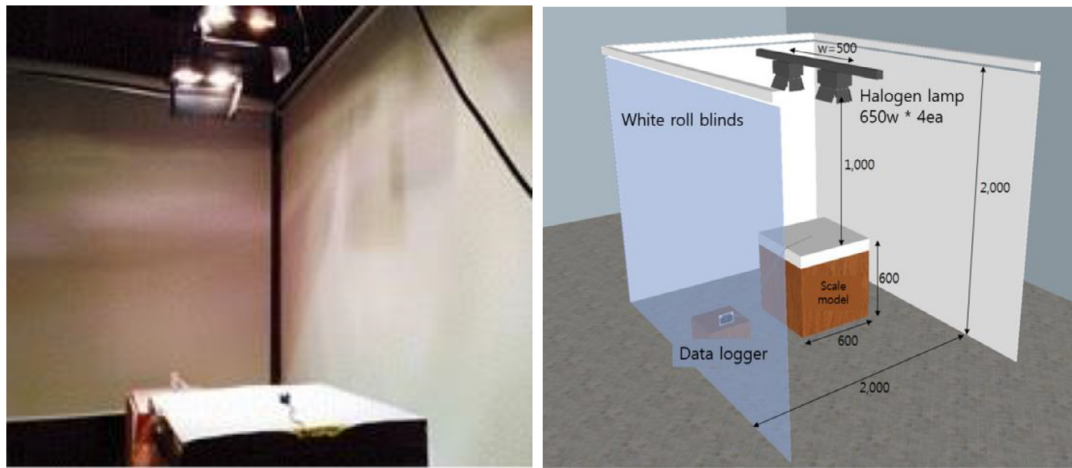


Fig. 5. Climatic chamber test.

Table 1
Comparison of standardized weather data with solar control stage.

Time		8	9	10	11	12	13	14	15	16	17	18	Total
Standardized weather data	Average value (W/m ²)	61	222	347	538	438	597	519	338	272	250	127	3709
Experimental data	Control value (W/m ²)	191 (Stage 1)	354 (Stage 2)	528 (Stage 3)	528 (Stage 3)	634 (Stage 4)	634 (Stage 4)	634 (Stage 4)	528 (Stage 3)	528 (Stage 3)	354 (Stage 2)	191 (Stage 1)	5104

Table 2
The species of PCM used in the experiment.

Plate finish color		PCM Melting point				
Finish color	White	Species of PCM	Bio 25	Bio 30	Bio 34	RT 44
Reflectivity	0.47	Melting point	25 °C	30 °C	34 °C	44 °C

cool roof, white water paint whose reflectance was 0.47 was applied to the WPC surface. There were four melting temperatures of the PCM used in the experiment: 25 °C, 30 °C, 34 °C, and 44 °C (see Table 2), all considering the mean temperatures of the four seasons in Seoul. For 25 °C, 30 °C, and 34 °C PCM, Bio-PCM in Phase Change Energy Solutions was used and for 44 °C PCM, n-Docosane series product of RUBITHERM® was used. The temperature measured portions were the surface of the WPC, the cavity space inside the WPC, and the indoor temperature in the scaled-down model.

2.3. Experimental conditions of the external test bed for performance verification

The PCM cool roof system was applied to the test bed implemented at an actual size to conduct the experiment for performance verification. The test bed consists of three rooms in total. The dimension of the rooms were 2500 mm × 2500 mm × 2500 mm. As for the internal finish, 100 mm of insulation panel was attached to minimize the effect from the external temperature. The test bed was composed of room 1 and room 2 which were in the experimental group, and room 3, which was the control group. Each room was configured as follows: Room1: WPC, Room2: WPC + PCM, Room3: WPC + PCM + Cool Paint (see Table 3., Fig 6–7). For the finish of the PCM cool roof system used in the experiment, WPC was determined through the “comparison experiment to select appropriate finishes as detailed in Section 2.1. The average wind speed and wind direction in Seoul is 2.3 m/s (The National Weather Service, 2017).

The performance verification using the test bed was conducted based on three seasons: spring, summer, and winter. Although

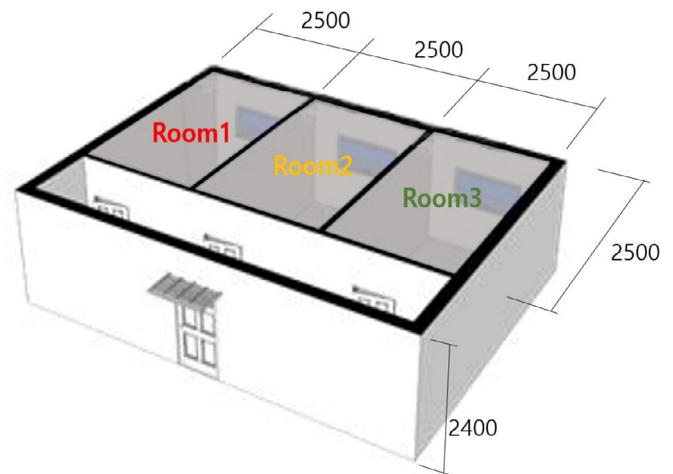


Fig. 6. Test-bed aerial view.

Seoul has four seasons; however since spring and autumn are similar in terms of climate characteristics, they were integrated into an “intermediate season” and spring was chosen for the measurement. The location of the test bed was at Chung-Ang University in Dongjak-gu, Seoul, Korea. For each season, measurements were conducted for 60 days. The detailed measurement period and climate status are summarized in Table 4.

Detailed analysis was conducted by selecting three consecutive sunny days without cloud cover as a representative value among the measurement data each season to analyze the performance of the PCM cool roof system accurately. The mean temperatures of

Table 3
Test-bed experiment overview.

Category	Contents		Test-bed floor plan
Height	2.5m		
Stories	1		
Direction	Southward		
Story height	2.4m		
Roof area	26m ²	Room1 6.25m ² Room2 6.25m ² Room3 6.25m ²	
Roof cladding	Room1	WPC	
	Room2	WPC+PCM	
	Room3	WPC+PCM+Cool Paint	

Table 4
Test-bed measurement period and weather conditions.

	Winter season	Middle season	Summer season
Location	Test bed at Rooftop Dept. of Engineering, Chung-Ang University, Heukseok-dong, Dongjak-gu, Seoul		
Total measurement period	'17.01.01 ~ '17.02.28	'17.03.01 ~ '17.04.30	'17.05.01 ~ '17.06.30
Date of detailed data analysis	01.14 ~ 01.16	03.01 ~ 04.30	06.14 ~ 06.16
Average temperature	4.8 °C	19.5 °C	26.8 °C
Average cloud cover	0	0.7	0.3
Average wind velocity	3.2 m/s	2.4 m/s	2.6 m/s



Fig. 7. Packing PCM inserted in WPC.

winter, spring, autumn and summer are 4.8 °C, 19.5 °C and 26.8 °C, respectively. The average wind speed and mean cloud are shown in Table 4 [26].

2.4. CFD analysis conditions for uhi mitigation effect

The analysis methods of the UHI can vary, and these include actual measurements, measurements of the thermal environment remotely, and scaled-down model tests, etc. However, there are various practical limitations, such as measurement costs and required human resources. Computer simulations have an advantage, in that they can analyze a wide range of circumstances and areas at a relatively lower cost. Thus, this study conducted a CFD simulation analysis according to the surface temperature of the building roof in an urban area to analyze the air current distribution and

Table 5
Simulation environment setting.

Item	Settings
Space	Three Dimensional
Mesh	Polyhedral Mesh
Mesh Size	0.05m
Time	Steady
Material	Gas
Flow	Segregated Flow
Fluid state	Equilibrium Air
Viscosity	Turbulent
Reynolds-turbulent flow	k-ε Turbulence
Iteration	100cycle

the occurrence of the heat island phenomenon in that urban area. For the initial values, the data derived from the summer testbed results were utilized.

The CFD simulation analysis program used in this study was Star-CCM+ (version 13.02) from CD-Adapco, and Table 5 summarizes the basic setup conditions for the CFD simulation. In this analysis, the standard k-ε model, which was first proposed by Launder and Spalding was employed. The mesh was set to 0.05 m in consideration of the target model and for the efficient operation of the simulation its shape was set to a polyhedral mesh, which is a hexagonal mesh that can be implemented in a three-dimensional (3D) analysis most effectively.

The air current analysis using the CFD in this study was a 3D turbulent compressive unsteady flow, and the governing equations were the fluid continuity equation, the momentum equation, the turbulent kinetic energy equation (k), and the turbulent dissipation energy equation (ε). As for the fluid flow, a numerical turbulence model should be applied, as the whole fluid field was regarded as a turbulent flow, based on the Reynolds number at the inlet, and the related governing equations regarding the physical

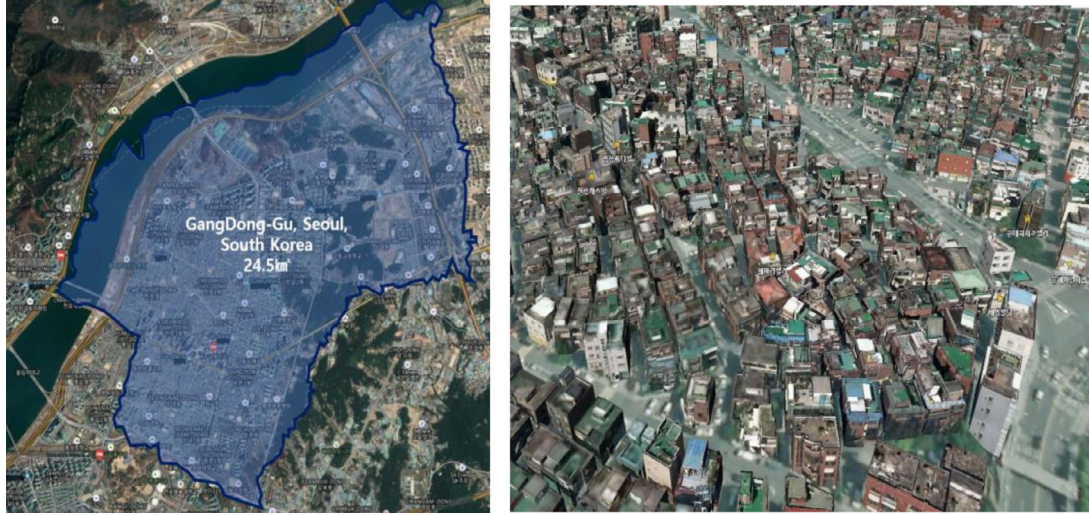


Fig. 8. Simulation analysis area - Gangdong-gu, Seoul, South Korea.

model relations were the continuity equation, the kinetic energy equation, the particle's motion equation, and the standard k- ϵ turbulence model equation, which are presented in Eq. (1)-(3).

$$\begin{aligned} \frac{\partial \rho}{\partial t} + \frac{\partial}{\partial x_i}(\rho u_i) &= S_m \\ \frac{\partial \rho u_i}{\partial t} + \frac{\partial}{\partial x_j}(\rho u_i u_j) &= -\frac{\partial p}{\partial x_j} + \frac{\partial \tau_{ij}}{\partial x_j} + \rho g_j + F_i \\ \tau_{ij} &= \left[\mu \left(\frac{\partial u_i}{\partial x_j} + \frac{\partial u_j}{\partial x_i} \right) \right] - \frac{2}{3} \mu \frac{\partial u_i}{\partial x_j} + \delta_{ij} \end{aligned} \quad (1)$$

$$\begin{aligned} \frac{du_p}{dt} &= \rho(u - u_p) + g(\rho_p - \rho)/\rho_p + F_x \\ F_D &= \frac{18\mu}{\rho_p D^2} \frac{C_D R_e}{24} \\ R_e &= \frac{\rho D_p |u_p - u|}{\mu} \\ C_D &= \alpha_1 + \alpha_2/Re + \alpha_3/Re^2 \end{aligned} \quad (2)$$

$$\begin{aligned} \frac{\partial}{\partial t}(\rho k) + \frac{\partial}{\partial x_j}(\rho u_j k) &= \frac{\partial}{\partial x_j} \left(\frac{\mu_t}{\sigma_k} \frac{\partial k}{\partial x_j} \right) + G_k + G_b - \rho \epsilon \\ \frac{\partial}{\partial t}(\rho \epsilon) + \frac{\partial}{\partial x_j}(\rho u_j \epsilon) &= \frac{\partial}{\partial x_j} \left(\frac{\mu_t}{\sigma_\epsilon} \frac{\partial \epsilon}{\partial x_j} \right) \\ &+ C_{1\epsilon} \frac{\epsilon}{k} (G_k + (1 - C_{3\epsilon})G_b) - C_{2\epsilon} \rho \frac{\epsilon^2}{k} \\ G_k &= \mu_t \left(\frac{\partial u_j}{\partial x_i} + \frac{\partial u_i}{\partial x_j} \right) \frac{\partial u_j}{\partial x_i} \\ G_b &= -g_i \frac{\mu_t}{\rho \sigma_h} \frac{\partial u_j}{\partial x_i} \\ C_{1\epsilon} &= 1.44, C_{2\epsilon} = 1.92, C_{3\epsilon} = 0.09, \sigma_k = 1.0, \sigma_\epsilon = 1.3 \end{aligned} \quad (3)$$

The study area was modeled around Gangdong-gu, Seoul, South Korea and CFD analysis was performed to analyze temperature distribution and airflow. Urban heat island phenomenon generally occurs in densely populated urban areas, and topography, altitude and building height are modeled using GIS in Gangdong-gu (Fig. 8). The total area of Gangdong-gu is 24.5 km² [27]. The residential area is modeled by applying the actual area as it is, and the commercial area is modeled by block because of the high building density. The wind speed was set at 3.6 m/s, which is the average wind

direction of the Seoul area in 2017 [26]. The simulation analysis setting is listed on Table 6.

3. Results

3.1. Results of thermal properties of materials

3.1.1. Measurements of heat conductivity by finishing materials

A study on the selection of appropriate finishes was conducted to select a material to be applied to the PCM cool roof system. The study results concluded that it is necessary for the PCM cool roof system to be manufactured as a packing type and for the roof to have a cavity space where the packing type PCM can be inserted. Thus, WPC, wood, and concrete were selected as the final finishes, excluding finishes that were relatively difficult to form a cavity space, and the heat conductivity of the three finishes was measured (see Table 7.).

However, a concrete roof required additional construction work, and therefore was not suitable to the PCM cool roof system whose advantage was that it was to be applied to existing buildings conveniently. Thus, concrete was excluded and general (hard and soft) wood was also excluded because it was relatively disadvantageous in terms of durability and strength. Thus, WPC was selected as the ideal finish and its detailed heat conductivity was measured.

3.1.2. Measurements of heat conductivity of the wpc in detail

Heat conductivity was measured through TCI analysis, and the mean of 10 t measurements showed its heat conductivity as 0.55 W/m·K and 0.53 W/m·K respectively when the cavity space was included or not. Table 8. presents heat conductivity when the cavity space is included and Table 9. presents heat conductivity measurement results when the cavity space is not included.

3.2. Results of the indoor artificial climate chamber test for selection a pcm type

To select a PCM appropriate to the climate of Seoul from the various PCMs according to a phase change temperature, PCMs whose phase change temperature was 25 °C, 30 °C, 34 °C, and 44 °C were applied to the scaled-down model to verify the thermal performance by simulating the climate in Seoul artificially in an artificial climate test room. The simulation results showed that a PCM of 44 °C was the most appropriate PCM for the climate in Seoul as

Table 6
Simulation Analysis Settings.

Setting temperature	Ambient setting temperature	26 °C (Summer)	
	Roof surface temperature	Normal roof surface temperature	33.1 °C
		PCM cool roof temperature	28.2 °C
Wind speed	3.6 m/s		
Wind direction	West		
Analysis area	Gangdong-gu, Seoul, Korea (24.5 km ²)		
Use district	Commercial & Residential		
Total roof area	39,143 m ²		
Building Average Height	31.5m		
Number of buildings	85		

Table 7
Thermal Conductivity Measurements by Finish Type.

Material	Thermal conductivity(W/m °C)
WPC	0.35
Hard wood	0.15
Soft wood	0.13
Normal concrete	1.83

Table 8
Results of WPC thermal conductivity measurement including hollow layer.

Measurement turn	Effusivity (Ws ² /m ² K)	k (W/mK)	1/m
1	887.9944	0.529941	96.88897
2	888.5313	0.530477	97.07762
3	889.8055	0.531175	96.99586
4	894.8415	0.536787	97.38058
5	890.3037	0.532248	97.11777
6	889.1223	0.531067	97.03074
7	893.0003	0.534945	97.3482
8	891.1271	0.533071	97.23239
9	894.2066	0.536152	97.3451
10	888.4203	0.530366	97.01608
-	Average	0.53268	-

Table 9
WPC thermal conductivity measurement results without hollow layer.

Measurement turn	Effusivity (Ws ² /m ² K)	k (W/mK)	1/m
1	899.1821117	0.541137	97.54179
2	906.0743065	0.548058	97.94915
3	913.4769912	0.555512	98.53692
4	906.1098626	0.548094	98.03331
5	908.2804648	0.550277	98.16699
6	911.3248005	0.553343	98.3449
7	915.3820019	0.557433	98.6515
8	911.1074731	0.553124	98.40718
9	911.2035677	0.553221	98.41604
10	913.5568462	0.555592	98.39406
-	Average	0.551579	-

all of the three temperature measured portions: WPC surface temperature (33.94 °C), cavity space temperature (32.94 °C), and indoor temperature (26.04 °C) in the scaled-down model had the lowest temperatures. A PCM whose phase change temperature was 44 °C and PCMs of other temperature showed temperature differences as follows: WPC surface: 0.67–1.53 °C, WPC cavity space: 0.35–0.68 °C, and indoor temperature in the scale-down model: 0.19–2.2 °C. For more details, refer to Fig. 9 to 11 and Table 10.

3.3. Result of the external test-bed for performance verification

3.3.1. Measurement results in winter

The measurement result on the mean surface temperature in the plate was as follows: WPC: -5.4 °C, WPC + PCM: -5.5 °C, WPC + PCM + Cool Paint: -7.9 °C. The measurement result on the mean internal temperature in the plate was as follows: WPC:

-6.1 °C, WPC + PCM: -5.2 °C, WPC + PCM + Cool Paint: -7.9 °C. The measurement results of the mean indoor temperature were as follows: WPC: 2.5 °C, WPC + PCM: 3.1 °C, WPC + PCM + Cool Paint: 3.6 °C (see Fig. 12–14, Table 11–13).

The mean surface temperature in the plate showed that Room 1, where only WPC was applied, had the highest temperature, and the mean indoor temperature showed that Room 3, where the PCM cool roof system was applied, had the highest temperature. Thus, the PCM cool roof system was proven to be effective in maintaining an indoor temperature due to the effects of the PCM, which not only had an effect on the reduction in surface temperature by increasing the reflectance of the surface, but also played a role as an insulator.

3.3.2. Measurement results in intermediate season

The measurement result on the mean surface temperature in the plate was as follows: WPC: 21 °C, WPC + PCM: 21.5 °C, WPC + PCM + Cool Paint: 16.8 °C. The measurement result on the mean internal temperature in the plate was as follows: WPC: 19.7 °C, WPC + PCM: 20.9 °C, WPC + PCM + Cool Paint: 14.9 °C. The measurement result on the mean indoor temperature was as follows: WPC: 17.4 °C, WPC + PCM: 17.6 °C, WPC + PCM + Cool Paint: 17.3 °C. The mean surface temperature in the plate showed that the temperature in Room 3 was the lowest. Thus, the PCM cool roof system can reduce a roof's surface temperature during the intermediate season, and conclusively, it can reduce the UHI. The indoor temperature showed a difference of 0.1 °C and 0.2 °C as compared to that of Room 1 and Room 2. This result indicated that a thermal equilibrium state was maintained without heat exchange according to the relationship of temperature between the indoor and outdoor and solar radiation (see Fig. 15–17, Table 14–16).

3.3.3. Measurement results in summer

The measurement result on mean surface temperature in the plate was as follows: WPC: 33.1 °C, WPC + PCM: 33.9 °C, WPC + PCM + Cool Paint: 28.2 °C. The measurement result on the mean internal temperature in the plate was as follows: WPC: 31.4 °C, WPC + PCM: 34.4 °C, WPC + PCM + Cool Paint: 26.5 °C. The measurement result on the mean indoor temperature was as follows: WPC: 25.9 °C, WPC + PCM: 26 °C, WPC + PCM + Cool Paint: 25.4 °C. The mean surface temperature on the plate and the mean indoor temperature showed that Room 3 where the PCM cool roof system was applied had the lowest temperature. Thus, the above results proved that when the PCM cool roof system was applied in summer, both of the reduction effects of roof's surface temperature and the indoor temperature (reduction in cooling load) were revealed (see Fig. 18–20, Table 17–19).

3.4. Results of cfd analysis conditions for uhi mitigation effect

This study conducted a CFD simulation analysis to analyze the occurrence of the UHI and the air current distribution according

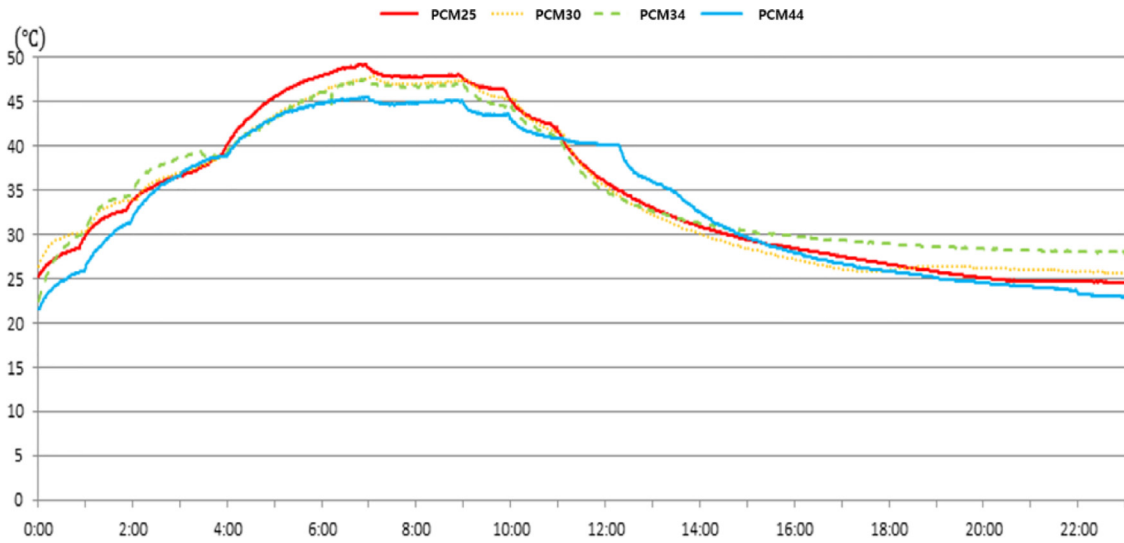


Fig. 9. WPC surface temperature.

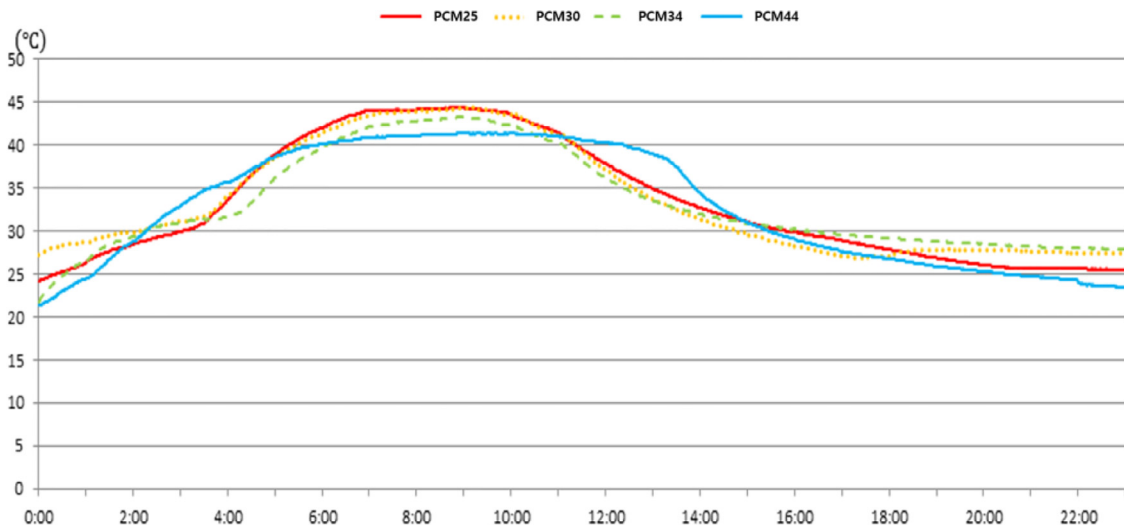


Fig. 10. WPC internal temperature.

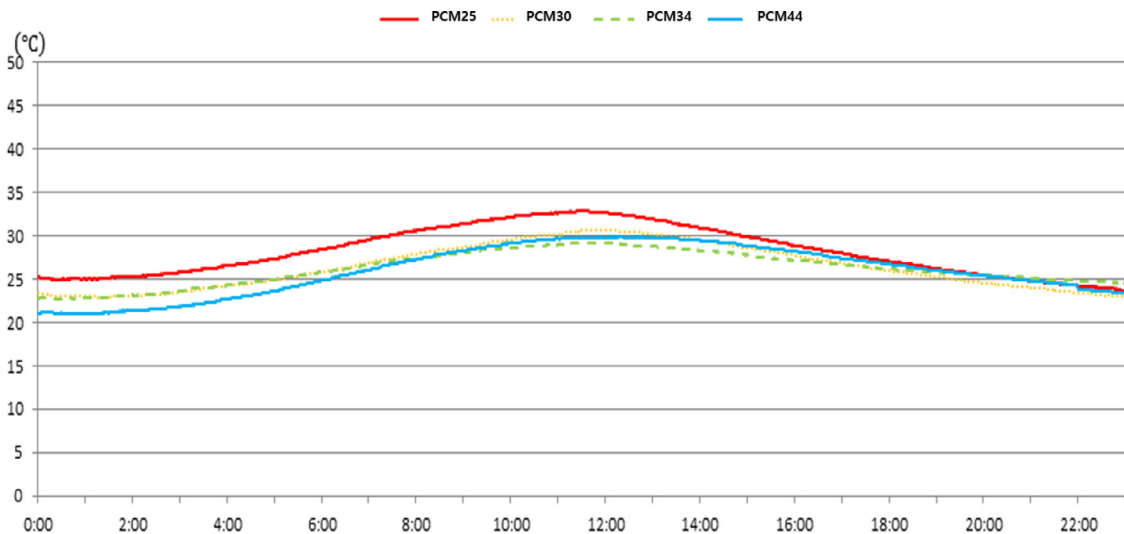


Fig. 11. Room temperature of scale model.

Table 10
Results of temperature comparison test by PCM type.

	Results of experiment by PCM type (Finish color: Reflectivity 0.47)			
	25 °C PCM	30 °C PCM	34 °C PCM	44 °C PCM
WPC surface temperature	34.87	34.61	35.47	33.94
WPC cavity temperature	33.43	33.62	33.29	32.94
Indoor temperature of Miniature model	28.24	26.44	26.23	26.04

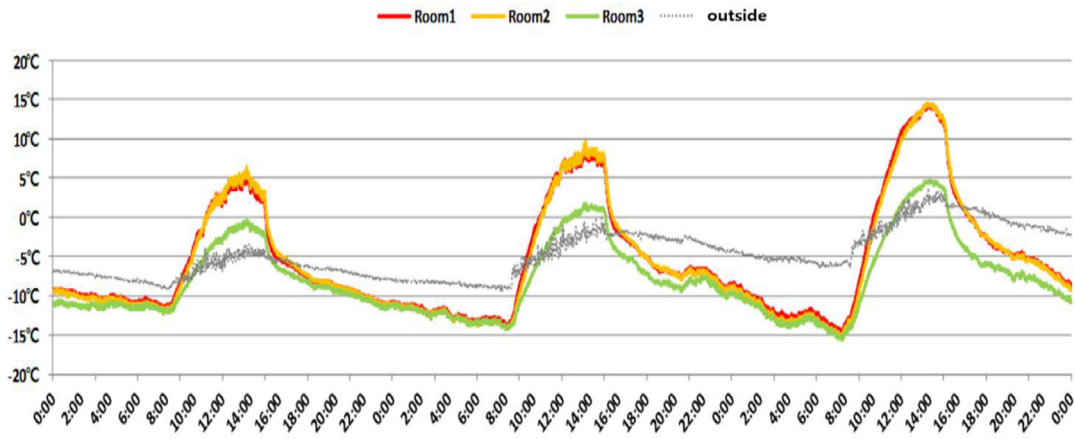


Fig. 12. Plate surface temperature per hour (winter).

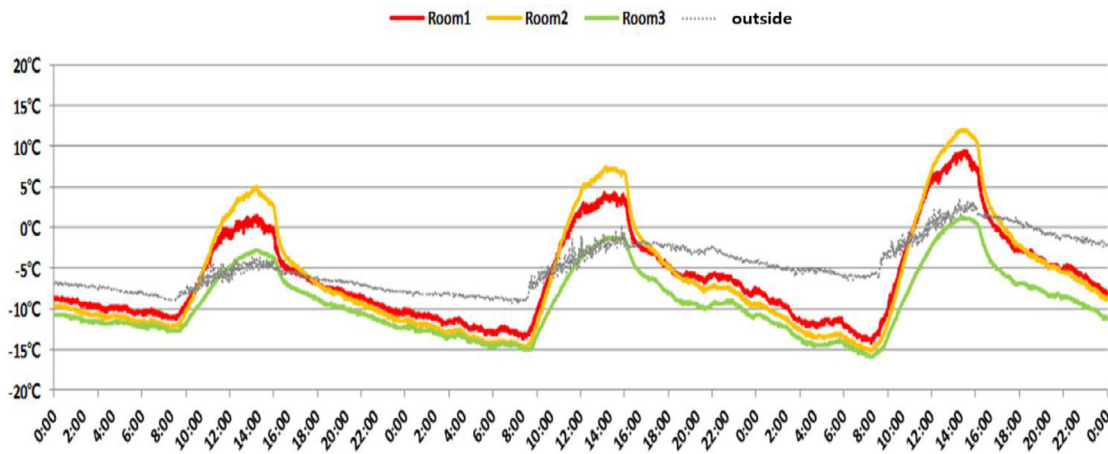


Fig. 13. Plate internal temperature per hour (winter).

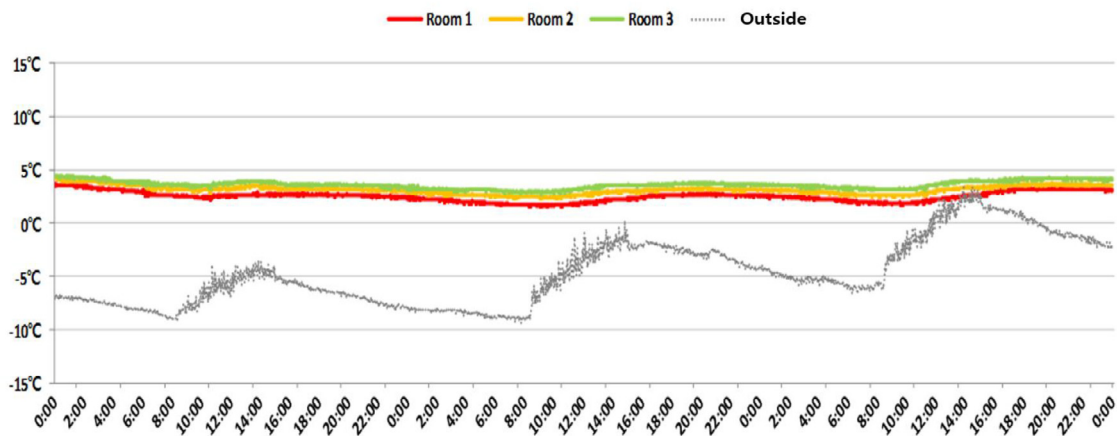


Fig. 14. Room temperature per hour of test-bed (winter).

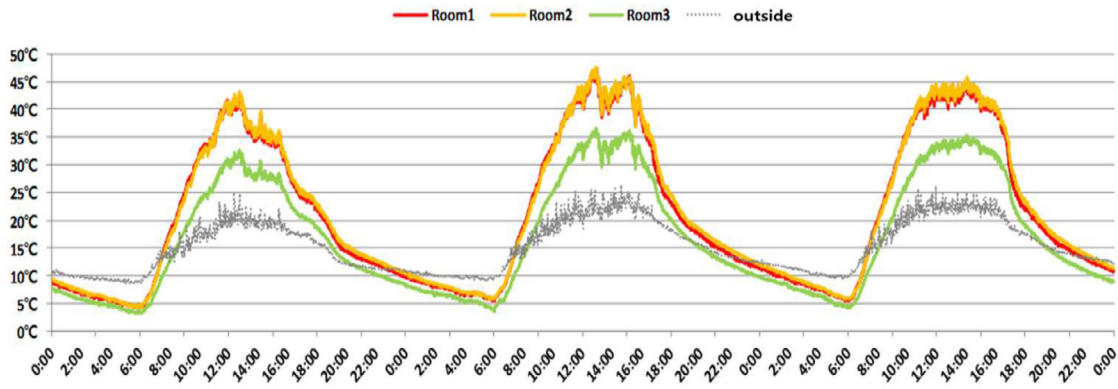


Fig. 15. Plate surface temperature per hour (intermediate season).

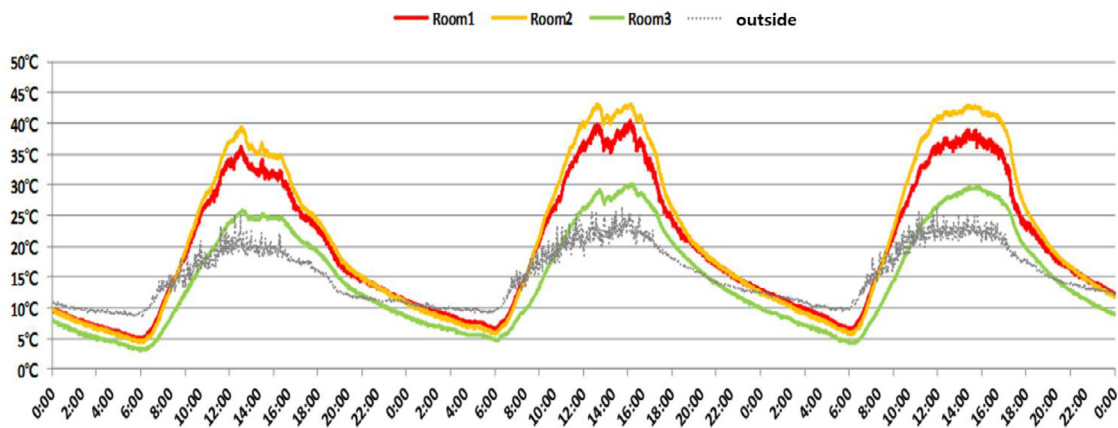


Fig. 16. Plate internal temperature per hour (intermediate season).

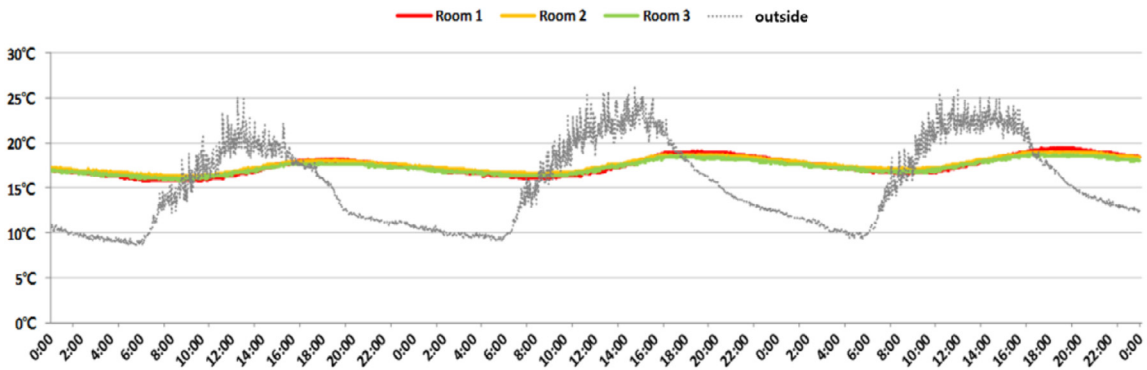


Fig. 17. Room temperature per hour of test-bed (intermediate season).

Table 11
Plate surface temperature results in winter (highest, lowest, average).

	Plate surface temperature		
	WPC	WPC+PCM	WPC+PCM+Cool Paint
Highest	14.3	14.6	4.7
Lowest	-14.6	-15.1	-15.5
Average	-5.4	-5.5	-7.9

Table 12
Plate internal temperature results in winter (highest, lowest, average).

	Plate internal temperature		
	WPC	WPC+PCM	WPC+PCM+Cool Paint
Highest	9.4	12.0	1.2
Lowest	-14.1	-15.2	-16.0
Average	-6.1	-5.2	-9.3

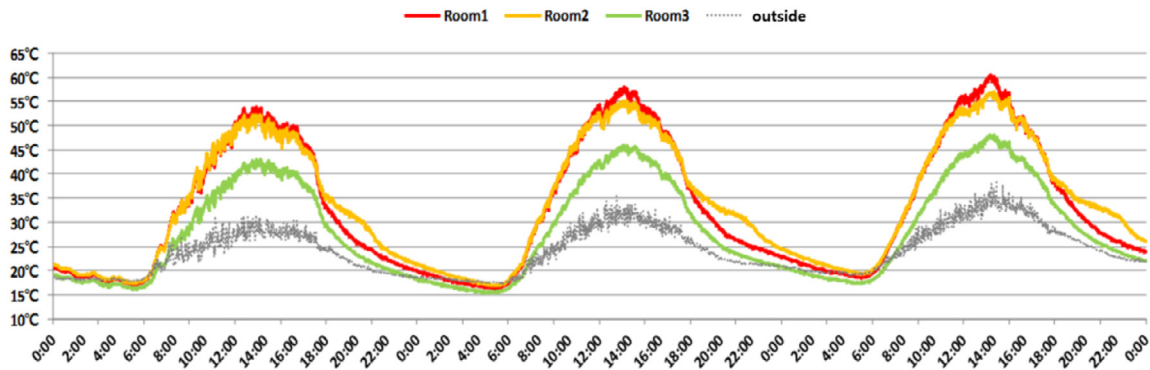


Fig. 18. Plate surface temperature per hour (summer).

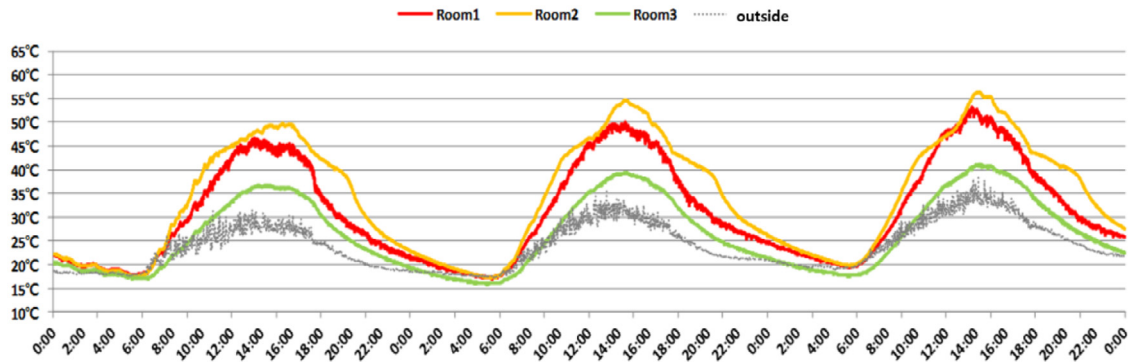


Fig. 19. Plate internal temperature per hour (summer).

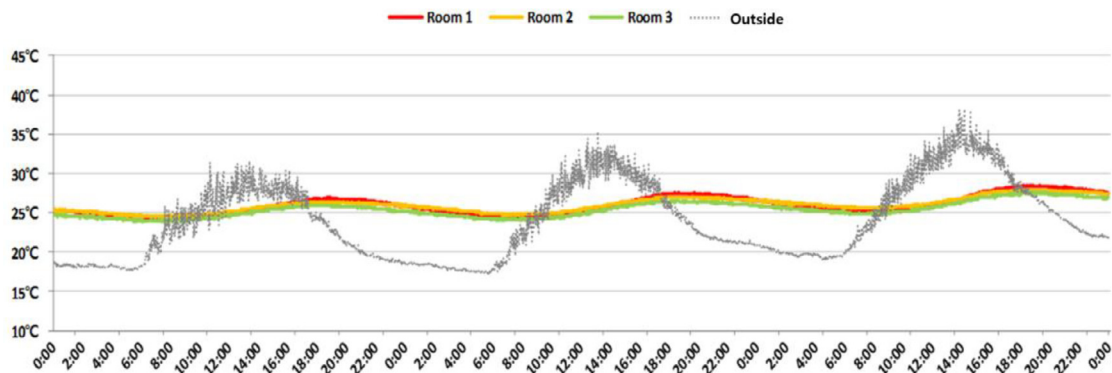


Fig. 20. Room temperature per hour of test-bed (summer).

Table 13
Results of the room temperature test-bed (winter).

	Indoor 1200 mm Temperature		
	WPC	WPC+PCM	WPC+PCM+Cool Paint
Highest	3.7	4.2	4.5
Lowest	1.6	2.4	2.8
Average	2.5	3.1	3.6

Table 14
Plate surface temperature results in intermediate season (highest, lowest, average).

	Plate surface temperature		
	WPC	WPC+PCM	WPC+PCM+Cool Paint
Highest	47.3	47.5	36.5
Lowest	4.3	4.4	3.3
Average	21.0	21.5	16.8

to changes in the surface temperature of the roof by the means of applying the PCM cool roof. The setup values were analyzed, as they were divided into two regions: the surface temperature of the general roof: (33.1 °C) and the surface temperature of the roof utilizing the PCM cool roof system: (28.2 °C).

3.4.1. Urban temperature analysis

The analysis results of the temperature distribution showed on Fig. 21 that the temperature in the urban canopy layer, which was 1 to 2 m above the roof surface, was higher than the outdoor air temperature (34–35 °C), thus verifying that the heat island phe-

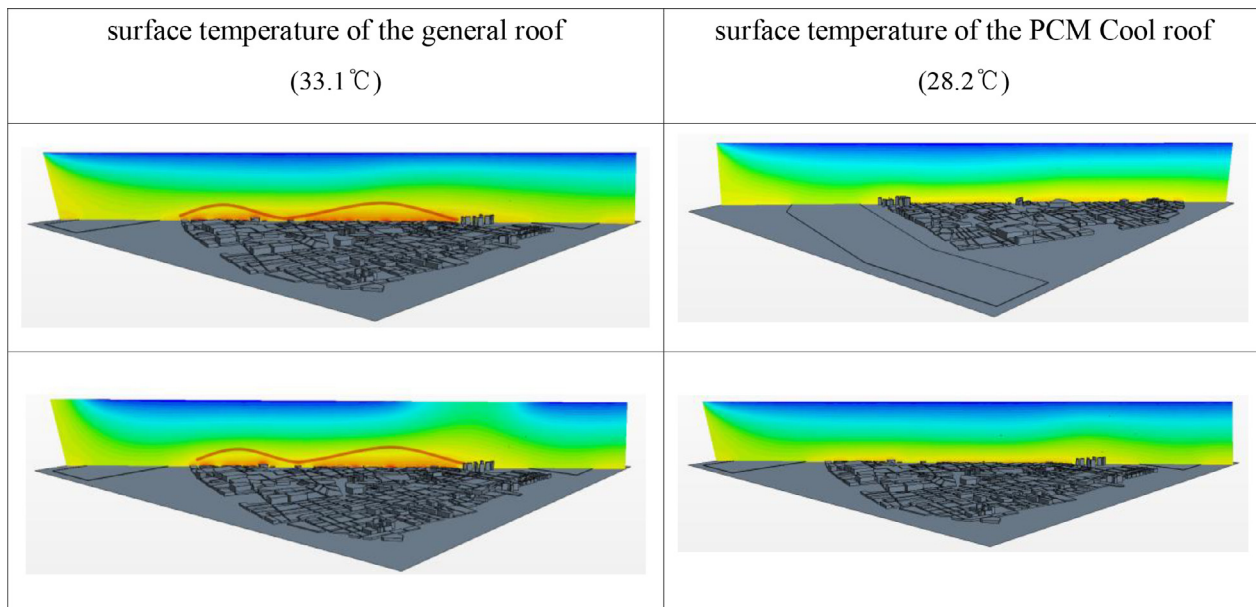


Fig. 21. Analysis of urban canopy layer temperature distribution.

Table 15

Plate internal temperature results in intermediate season (highest, lowest, average).

	Plate internal temperature		
	WPC	WPC+PCM	WPC+PCM+Cool Paint
Highest	40.5	43.2	30.1
Lowest	5.0	4.5	3.1
Average	19.7	20.9	14.9

Table 16

Results of the room temperature test-bed (intermediate season).

	Indoor 1200 mm temperature		
	WPC	WPC+PCM	WPC+PCM+Cool Paint
Highest	19.4	19.0	18.7
Lowest	15.8	16.2	15.9
Average	17.4	17.6	17.3

Table 17

Plate surface temperature results in summer (highest, lowest, average).

	Plate surface temperature		
	WPC	WPC+PCM	WPC+PCM+Cool Paint
Highest	60.5	57.1	48.1
Lowest	16.2	16.8	15.4
Average	33.1	33.9	28.2

nomenon occurs. In contrast, the temperature of the roof surface in the urban area where the PCM cool roof system was applied and the temperature distribution at 1–2 m height, and that of a height of 10 m were lower (27–29 °C) and more evenly distributed.

3.4.2. Air current analysis. As shown in Fig. 22, the analysis results of the air current distribution verified that the temperatures in the urban area where the general roof was applied showed that the air currents did not spread to the suburban areas, but remained in the urban area, while conversely in the urban area where the PCM cool roof system was applied the air currents spread to the suburban areas.

Table 18

Plate internal temperature results in summer (highest, lowest, average).

	Plate internal temperature		
	WPC	WPC+PCM	WPC+PCM+Cool Paint
Highest	53.3	56.4	41.2
Lowest	17.2	17.2	16.0
Average	31.4	34.4	26.5

Table 19

Results of the room temperature test-bed (summer).

	Indoor 1200 mm temperature		
	WPC	WPC+PCM	WPC+PCM+Cool Paint
Highest	28.5	27.9	27.5
Lowest	24.1	24.5	23.9
Average	25.9	26.0	25.4

4. Discussion

This study verified the reduction of roof surface temperatures in buildings using the PCM cool roof system. As in prior studies, this study conducted by the urban scaled-down models, site measurements, and computer simulations. The roof's surface temperature was analyzed through a test bed that simulated an actual building to determine the effect of reduction in the UHI ultimately. Furthermore, this study conducted the verification of the effect on the reduction in the cooling load of buildings by analyzing the indoor temperature in the test bed where the PCM cool roof system was applied.

The study procedure had the following steps: Step 1: selection of appropriate candidates of roof finishes, Step 2: selection of PCM whose phase change temperature is appropriate for the climate of Seoul, and Step 3: comparison and verification of reduction effects of the surface temperature in the roof's finish and the indoor temperature in the PCM cool roof system. The study results are as follows.

The heat conductivity of WPC, wood, and concrete that can form a cavity space with appropriate strength was measured, and

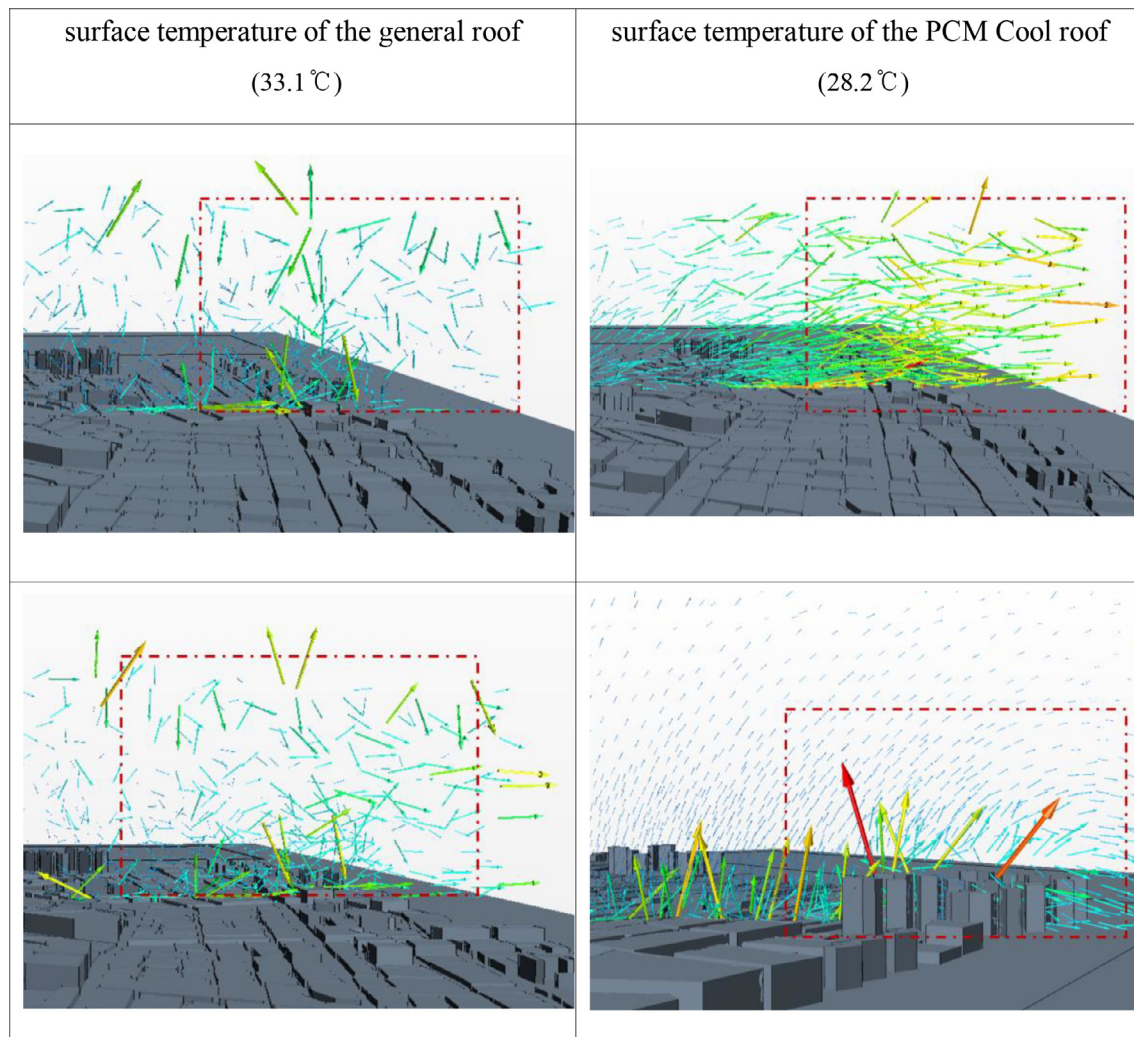


Fig. 22. Analysis of airflow distribution in the city.

the result showed that WPC for each finish was: 0.35 W/m °C, hard wood: 0.15 W/m °C, soft wood: 0.13 W/m °C, and ordinary concrete: 1.83 W/m °C. However, concrete that required additional construction work was excluded because it was relatively difficult to for a PCM to be applied to existing buildings, Wood, whose durability and strength was weak was also excluded. Thus, WPC was selected as the ideal finish as appropriate and its detailed heat conductivity was measured.

A scaled-down model was constructed to select a PCM that was appropriate for the climate of Seoul and the thermal performance was verified in the artificial climate test room that simulated the climate of Seoul during the summer. The performance result exhibited the lowest temperature in the temperature measured portions occurred with a PCM that had a 44 °C phase change temperature. Thus, it was selected as the most appropriate PCM for the climate of Seoul. The surface temperature in each portion was as follows: surface temperature at the WPC: 33.94 °C, temperature at the cavity space: 32.94 °C, indoor temperature in the scale-down model: 26.04 °C.

For the test bed applied performance verification to analyze the reduction effect of the roof's surface temperature, the test period was divided into three seasons: winter, spring (intermediate season), and summer. For each season, measurements were conducted for 60 days. The detailed analysis was conducted by select-

Table 20

Seasonal roof surface temperature measurements of test-bed.

	Room1(WPC)	Room2(WPC +PCM)	Room3(WPC +PCM+Cool Paint)
Winter season	-5.4 °C	-5.5 °C	-7.9 °C
Middle season	21 °C	21.5 °C	16.8 °C
Summer season	33.1 °C	33.9 °C	28.2 °C

ing three consecutive sunny days as representative data. The measurement results in winter verified that the PCM cool roof system was proven to reduce the roof's surface temperature and maintain the indoor temperature as the PCM played a role as an insulator.

The reduction effect of roof's surface temperature by the PCM cool roof system was also verified in the intermediate season as well. Both the reduction effect of roof's surface temperature and the indoor temperature (reduction in cooling load) were also verified during summer. The roof's surface temperature for each season is as follows(see Table 20).

The analysis results of the temperature distribution in the urban area utilizing the CFD, verified that the temperature of the roof

surface in an urban area where a PCM cool roof system was applied was lower than that of a general roof. In particular, the temperature distribution at 1 to 2 m height, which was defined as the urban canopy layer, was lower and more evenly distributed when the PCM cool roof system was applied. Due to this temperature distribution, the urban area where the PCM cool roof system was applied had air currents that spread to the suburban areas from the urban area.

5. Conclusion

This study verified the effects on the reduction of the UHI through the performance verification of roof surface temperatures in building using a PCM cool roof system. Prior to this study, urban scaled-down models and site measurement studies were conducted considering only preliminary studies. This study analyzed the effects on the reduction of the heat island and the associated reduction in roof surface temperatures through a testbed application that simulated an actual building, as well as utilizing CFD analysis. Furthermore, this study conducted the verification of the effects on the reduction in the cooling loads in buildings by analyzing the indoor temperature in the testbed, where the PCM cool roof system was applied to promote building energy saving.

Results showed that it was appropriate to select a material whose durability and strength were strong, and has heat conductivity, such as WPC in order to effectively apply the PCM to the roof surface. The most suitable PCM product used for the climate of Seoul is one whose phase change temperature is 44 °C. As described above, the PCM cool roof system was fabricated and applied to the roof surface of the testbed. The application results showed an effect on the reduction of the surface temperature of -4.9 °C on average. The CFD analysis results, based on the above data, verified that the UHI was reduced, and the air currents previously restricted to the urban areas, actively spread to the suburban areas, thereby preventing the deterioration of air quality in urban areas, due to the reduction of spreading of fine dust and automobile exhaust.

As presented in the above, the maximum difference in roof's surface temperature for each season was: winter: 2.5 °C, intermediate season: 4.7 °C, and summer: 5.7 °C. The above result verified the effect on the reduction in the UHIP based on the previous study by Oke et al. [28], suggesting that "the UHIP should be investigated based on temperatures at the urban canopy layer that is corresponded to 1–2 m height (screen level) from the ground". This study developed a PCM cool roof system appropriate for the climate of Seoul, Korea, and proved the effect of reduction in UHI through performance verification. The study results are expected to be utilized as foundational data to be used to reduce the UHI in the future.

Declaration of Competing Interest

This research was supported by the Chung-Ang university research scholarship grants in 2019.

Supplementary materials

Supplementary material associated with this article can be found, in the online version, at doi:[10.1016/j.enbuild.2019.109537](https://doi.org/10.1016/j.enbuild.2019.109537).

References

- [1] W.P. Lee, Basic Geography terminology Dictionary For High Schooler, Shinwon Publishing Co, 2002.
- [2] L.M. Gartland, Heat islands: Understanding and Mitigating Heat in Urban Areas, Routledge, 2012.
- [3] K.S. Oh, J.J. Hong, The relationship between urban spatial elements and the urban heat island effect, *Journal of the Urban Design Institute of Korea Urban Design* 6 (1) (2005) 47–63.
- [4] J.R. Jeong, M.H. Chung, J.C. Park, Thermal performance of roof surface reflectance in urban areas for mitigation of urban heat island effect, *Journal of The Architectural Institute of Korea Structure & Construction* 33 (5) (2017) 73–79.
- [5] Y. Song, Influence of new town development on the urban heat island-the case of the bundang area, *J Environ Sci (China)* 17 (4) (2005) 641–645.
- [6] T.M. Gál, Z. Sümeghy, Mapping the roughness parameters in a large urban area for urban climate applications, *Acta Climatologica ET Chorologica* 40 (2007) 27–36.
- [7] H.C. Kim, S.K. Choi, B.R. Yun, A statistical analysis on temperature change and climate variability in Korea, *Communications for Statistical Applications and Methods* 18 (1) (2011) 1–12.
- [8] Parkmungak, Current Events Summary Message Photo, Parkmungak, 2013.
- [9] I. Saito, O. Ishihara, T. Katayama, Study of the effect of green areas on the thermal environment in an urban area, *Energy Build* 15 (3–4) (1990) 493–498.
- [10] Y. Kim, D.H. Kang, K.H. Ahn, Characteristics of urban heat-island phenomena caused by climate changes in Seoul, and alternative urban design approaches for their improvements, *J. Urban Des. Inst. Korea* 12 (2011) 5–14.
- [11] Y. Ohashi, T. Ihara, Y. Kikegawa, N. Sugiyama, Numerical simulations of influence of heat island countermeasures on outdoor human heat stress in the 23 wards of Tokyo, Japan, *Energy Build* 114 (2016) 104–111.
- [12] M. Kolokotroni, R. Giridharan, Urban heat island intensity in London: an investigation of the impact of physical characteristics on changes in outdoor air temperature during summer, *Solar Energy* 82 (11) (2008) 986–998.
- [13] S.H. Park, K.B. Kong, H.J. Min, Performance evaluation of cool roof for mitigating urban heat island effects - Case study of "GangNam-gu public health center" in Seoul, South Korea -. *Journal of the Architectural Institute of Korea Structure & Construction* 33 (4) (2017) 55–62.
- [14] H.C. Yun, M.G. Kim, K.Y. Jung, Analysis of temperature change by forest growth for mitigation of the urban heat island, *Journal of the Korean Society of Surveying, Geodesy, Photogrammetry and Cartography* 31 (2) (2013) 143–150.
- [15] J.M. Chun, S.Y. Lee, K.R. Kim, Y.J. Choi, A study of the urban heat island in Seoul using local analysis system, *Journal of Korean Society for Atmospheric Environment* 30 (2) (2014) 119–127.
- [16] M.H. Chung, J.C. Park, Development of PCM cool roof system to control urban heat island considering temperate climatic conditions, *Energy Build* 116 (2016) 341–348.
- [17] Y.K. Yang, I.S. Kang, M.H. Chung, S.M. Kim, J.C. Park, Effect of PCM cool roof system on the reduction in urban heat island phenomenon, *Building and Environment* 122 (2017) 411–421.
- [18] T. Karlessi, M. Santamouris, A. Synnefa, D. Assimakopoulos, P. Didaskalopoulos, K. Apostolakis, Development and testing of PCM doped cool colored coatings to mitigate urban heat island and cool buildings, *Building and Environment* 46 (3) (2011) 570–576.
- [19] E. Ripley, O. Archibald, D. Bretell, Temporal and spatial temperature patterns in Saskatoon, *Weather* 51 (12) (1996) 398–405.
- [20] A.J. Arnfield, Two decades of urban climate research: a review of turbulence, exchanges of energy and water, and the urban heat island, *International journal of climatology* 23 (1) (2003) 1–26.
- [21] J.A. Voogt, T.R. Oke, Thermal remote sensing of urban climates, *Remote Sens Environ* 86 (3) (2003) 370–384.
- [22] K. Uehara, Wind tunnel experiments on how thermal stratification affects flow and dispersion within and above urban street canyons, *Wind Engineers, JAWE* 1998 (75) (1998) 37–42.
- [23] F.S. de la Flor, S.A. Dominguez, Modelling microclimate in urban environments and assessing its influence on the performance of surrounding buildings, *Energy Build* 36 (5) (2004) 403–413.
- [24] P.A. Mirzaei, F. Haghghat, Approaches to study urban heat island-abilities and limitations, *Building and Environment* 45 (10) (2010) 2192–2201.
- [25] K.K. Roman, T. O'Brien, J.B. Alvey, O. Woo, Simulating the effects of cool roof and PCM (phase change materials) based roof to mitigate UHI (urban heat island) in prominent US cities, *Energy* 96 (2016) 103–117.
- [26] T.N.W. Service, Direction and velocity of wind data statistics. 2017 [cited 2016 11.18]; Available from: <http://www.kma.go.kr>.
- [27] M.O. Land, National spatial data distribution system V-world map service. 2017 [cited 2016 11.18]; Available from: <http://map.vworld.kr>.
- [28] T.R. Oke, Street design and urban canopy layer climate, *Energy Build* 11 (1–3) (1988) 103–113.